Disruption of IGF-1R signaling by a novel quinazoline derivative, HMJ-30, inhibits invasiveness and reverses epithelial-mesenchymal transition in osteosarcoma U-2 OS cells

YU-JEN CHIU[1,2*], MANN-JEN HOUR[3*], YI-AN JIN[4], CHI-CHENG LU[5], FUU-JEN TSAI[6-8], TAI-LIN CHEN[9], HSU MA[1,2,10], YU-NING JUAN[11] and JAI-SING YANG[11]

[1]Division of Plastic and Reconstructive Surgery, Department of Surgery, Taipei Veteran General Hospital; [2]Department of Surgery, School of Medicine, National Yang Ming University, Taipei 112; [3]School of Pharmacy, China Medical University, Taichung 404; [4]Department of Dermatology, Taipei Medical University Hospital, Taipei 110; [5]Department of Pharmacy, Buddhist Tzu Chi General Hospital, Hualien 970; [6]Genetics Center, Department of Medical Research, China Medical University Hospital; [7]School of Chinese Medicine, China Medical University; [8]Department of Medical Genetics, China Medical University Hospital, Taichung 404; [9]Institute of Biochemistry and Molecular Biology, National Yang Ming University, Taipei 112; [10]Department of Surgery, National Defense Medical Center, Taipei 114 [11]Department of Medical Research, China Medical University Hospital, China Medical University, Taichung 404, Taiwan, R.O.C.

Abstract. Osteosarcoma is the most common primary malignancy of the bone and is characterized by local invasion and distant metastasis. Over the past 20 years, long-term outcomes have reached a plateau even with aggressive therapy. Overexpression of insulin-like growth factor 1 receptor (IGF-1R) is associated with tumor proliferation, invasion and migration in osteosarcoma. In the present study, our group developed a novel quinazoline derivative, 6-fluoro-2-(3-fluorophenyl)-4-(cyanoanilino)quinazoline (HMJ-30), in order to disrupt IGF-1R signaling and tumor invasiveness in osteosarcoma U-2 OS cells. Molecular modeling, immune-precipitation, western blotting and phosphorylated protein kinase sandwich ELISA assays were used to confirm this hypothesis. The results demonstrated that HMJ-30 selectively targeted the ATP-binding site of IGF-1R and inhibited its downstream phosphoinositide 3-kinase/protein kinase B, Ras/mitogen-activated protein kinase, and IκK/nuclear factor-κB signaling pathways in U-2 OS cells. HMJ-30 inhibited U-2 OS cell invasion and migration and downregulated protein levels and activities of matrix metalloproteinase (MMP)-2 and MMP-9. An increase in protein levels of tissue inhibitor of metalloproteinase (TIMP)-1 and TIMP-2 was also observed. Furthermore, HMJ-30 caused U-2 OS cells to aggregate and form tight clusters, and these cells were flattened, less elongated and displayed cobblestone-like shapes. There was an increase in epithelial markers and a decrease in mesenchymal markers, indicating that the cells underwent the reverse epithelial-mesenchymal transition (EMT) process. Overall, these results demonstrated the potential molecular mechanisms underlying the effects of HMJ-30 on invasiveness and EMT in U-2 OS cells, suggesting that this compound deserves further investigation as a potential anti-osteosarcoma drug.

Introduction

Osteosarcoma is the most common primary malignancy of the bone in adolescents and is characterized by local invasion and distant metastasis (1). The survival rate has improved with the use of multi-agent chemotherapy, from 11% with surgical resection alone in the 1960s to 70% with the addition of chemotherapy by the mid-1980s (2). However, long-term outcomes have reached a plateau over the past 20 years (3). Tumor progression to the invasive and metastatic states increases morbidity and mortality in cancer and represents the most formidable obstacle to successful treatment (4). Overall, ~30% of patients with a localized form of the disease and 80% of patients with a metastatic form of the disease at the point of initial diagnosis will relapse. These patients

Correspondence to: Dr Jai-Sing Yang, Department of Medical Research, China Medical University Hospital, China Medical University, 2 Yude Road, Taichung 40447, Taiwan, R.O.C.
E-mail: jaisingyang@gmail.com

*Contributed equally

cannot be described as cured, and they have <20% chance of long-term survival despite aggressive therapies. Conventional chemotherapies frequently induce drug-resistance and cause severe side effects (5,6). For these reasons, novel therapies are required to treat patients with osteosarcomas.

Insulin-like growth factor 1 receptor (IGF-1R) belongs to the large class of tyrosine kinase receptors that are activated by IGF-1 and by the associated growth factor IGF-2. The ligand-receptor interaction initiates receptor autophosphorylation of tyrosine residues and subsequently activates multiple signalling pathways, including the mitogen-activated protein kinase (MAPK) and phosphoinositide 3-kinase (PI3K) signaling pathways (7). IGF-1R has been demonstrated to be not only a key regulator of normal physiological cell processes, but also to serve important functions in carcinogenesis and tumor development, including tumor growth, progression, invasion and metastasis (8-10).

The IGF system is an important regulator of bone formation and homeostasis (11). During the adolescent growth spurt, elevated levels of IGF-1 coincide with a high prevalence of osteosarcoma, suggesting that IGF-1 may contribute to the pathogenesis of osteosarcoma (5,12). Previous studies have reported that human osteosarcoma cell lines display functional IGF-1R on their surface (13,14). In human primary osteosarcoma tissue samples, the levels of IGF-R, IGF-1, and IGF-2 were increased compared with positive control cell lines (15,16). *In vitro*, inhibition of growth and invasiveness may result from downregulation of IGF-IR (14,17). Furthermore, IGF-1R blockade increases radio-sensitivity and induces apoptosis in multidrug-resistant osteosarcoma cell lines (5,14). These results suggest that compounds which specifically inhibit the function of IGF-1R tyrosine kinase in cancer cells may potentially be an effective treatment strategy. Early studies have revealed that analogues of and antagonists to growth hormone-releasing hormone decrease serum IGF-1 levels and inhibit tumor growth in mice, but failed in their phase 1 clinical trial (18,19). An alternative approach has been to block the interaction of IGF-1R with IGF-1 and IGF-2 by targeting IGF-1R, and, most importantly, to downregulate the receptor by internalization and degradation via the endosome (20). In the present study, our group developed a novel quinazoline derivative, 6-fluoro-2-(3-fluorophenyl)-4-(cyanoanilino)quinazoline (HMJ-30; Fig. 1A), to disrupt IGF-IR signaling and inhibit tumor invasion and migration in osteosarcoma cells.

Epithelial-mesenchymal transition (EMT) is a program of biological development in which cells lose their epithelial characteristics and gain mesenchymal properties during embryogenesis, as well as for the maintenance of homeostasis and the architecture of epithelial structures during adult life (21). EMT is controlled by receptor tyrosine kinase pathways (22). Over the last decade, accumulating evidence has suggested that EMT regulated by similar pathways is recapitulated during solid tissue epithelial cancer progression and invasion, thereby contributing to the formation of metastases (23). Mesenchymal-epithelial transition (MET) is the reverse of EMT, and serves an important function in the formation of somites and in kidney morphogenesis. This reverse process is characterized by cytoskeletal reorganization with the reactivation of epithelial cell markers and the loss of

mesenchymal cell markers (24). However, relevant literature is comparatively rare, particularly concerning cancer.

Quinazoline derivatives have diverse pharmacological properties, including anti-microbial, anti-malarial, analgesic, sedative, hypoglycemic, anti-tubercular and anticancer activities (25). In the past 10 years, a large number of experimental studies have demonstrated that novel quinazoline derivatives are able to selectively inhibit important pathways through blocking growth factor receptors, including epithelial growth factor receptor, vascular endothelial growth factor, platelet-derived growth factor, ErbB2 and c-Src (26-30). One of the most well-characterized derivatives is gefitinib (Iressa), which is the first selective inhibitor of epidermal growth factor receptor that binds to the adenosine triphosphate (ATP)-binding site of the receptor to deter non-small cell lung cancer (31). There are no reports on quinazoline derivatives targeting IGF-1R, or concerning the potential anticancer effects. Our group recently designed and synthesized quinazoline series compounds, and one of these compounds, HMJ-30, presented in Fig. 1A, may be a novel anti-IGF-1R agent (32,33). The present study investigated the novel quinazoline derivative HMJ-30, which inhibits invasiveness in U-2 OS cells, and elucidated the potential signaling pathways.

Materials and methods

Chemicals. HMJ-30 was designed and synthesized by Dr Mann-Jen Hour (School of Pharmacy, China Medical University, Taichung, Taiwan). Dimethyl sulfoxide (DMSO), potassium phosphate, trypan blue, propidium iodide (PI), Triton X-100, Tris-HCl, MTT and ribonuclease-A were obtained from Sigma-Aldrich; Merck KGaA (Darmstadt, Germany). McCoy's 5a medium, L-glutamine, fetal bovine serum (FBS), trypsin-EDTA, penicillin G and streptomycin were obtained from Gibco; Thermo Fisher Scientific (Waltham, MA, USA). Antibodies against phosphorylated (p-) protein kinase B (AKT) (cat. no. 4060), AKT (cat. no. 4691), p-extracellular signal-regulated kinase (ERK) (cat. no. 4370), ERK (cat. no. 4695), p-c-Jun amino-terminal kinase (JNK) (cat. no. 4668), JNK (cat. no. 9252), p-p38 (cat. no. 4511), p38 (cat. no. 8690), p-IGF-1R β (Tyr1131)/insulin receptor β (IRβ; Tyr1146) (cat. no. 3021), and Ras (cat. no. 3965) were purchased from Cell Signaling Technology, Inc. (Danvers, MA, USA). Antibodies against β-actin (cat. no. sc-47778), α-tubulin (cat. no. sc-5286), IGF-1R (cat. no. sc-9038), IR (cat. no. sc-710), PI3K (p85) (cat. no. sc-1637), IKK (cat. no. sc-7607), nuclear factor-κB (NF-κB; p65) (cat. no. sc-372), p-IκB (cat. no. sc-8404), IκB (cat. no. sc-371), matrix metalloproteinase (MMP)-2 (cat. no. sc-13595), MMP-9 (cat. no. sc-21733), tissue inhibitor of metalloproteinase (TIMP)-1 (cat. no. sc-5538), TIMP-2 (cat. no. sc-5539), and all goat anti-mouse (cat. no. sc-2005) and anti-rabbit (cat. no. sc-2004) immunoglobulin (IgG)-horseradish peroxidase (HRP) secondary antibodies were purchased from Santa Cruz Biotechnology, Inc. (Dallas, TX, USA). Epithelial cadherin (E-cadherin) (cat. no. 07-697), β-catenin (cat. no. 05-613), fibronectin (cat. no. CP70) and vimentin (cat. no. CBL202) primary antibodies were from EMD Millipore (Billerica, MA, USA). Materials and chemicals for electrophoresis were obtained from Bio-Rad Laboratories, Inc. (Hercules, CA, USA).
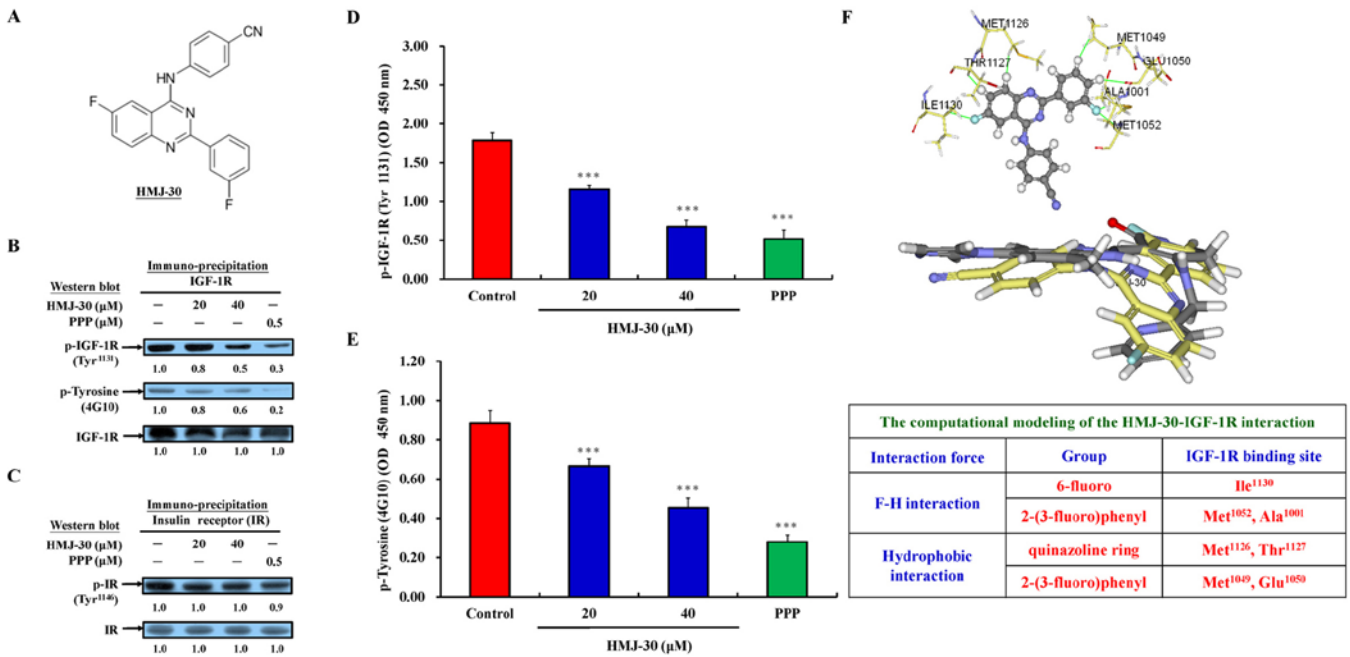
Figure 1. HMJ-30 selectively targets the IGF-1R ATP binding site. (A) The chemical structure of HMJ-30. (B) Following treatment with 0, 20, and 40 μM HMJ-30 for 6 h, U-2 OS cells were harvested and total proteins were collected. IGF-1R was evaluated by immune-precipitation and p-IGF-1R (Tyr[1131]) and p-tyrosin (4G10) were evaluated by western blotting. (C) Following treatment with 0, 20 and 40 μM HMJ-30 or with PPP for 6 h, cells were harvested and total proteins were collected. IR was evaluated by immune-precipitation, and p-IR (Tyr[1146]) was evaluated by western blotting. (D) p-IGF-1R (Tyr 1131) protein levels were evaluated by ELISA. (E) Tyrosine kinase activity was evaluated using a tyrosine kinase assay. (F) In order to predict the major target site of HMJ-30 to IGF-1R, the docking simulation of HMJ-30 and IGF-1R was performed using a computational modeling program. The interactions reveal that HMJ-30 binds readily to the ATP-binding site of IGF-1R with low potential energy. The superimposed image is of HMJ-30 (yellow color) and benzimidazole inhibitor A (gray color). The data represents the mean ± standard deviation of three experiments. ***P<0.001 vs. control. HMJ-30, 6-fluoro-2-(3-fluorophenyl)-4-(cyanoanilino) quinazoline; IGF-1R, insulin-like growth factor 1 receptor; ATP, adenosine trisphosphate; p-, phosphorylated; PPP, picropodophyllotoxin; IR, insulin receptor.

Cell culture. U-2 OS, a human osteogenic sarcoma cell line, was obtained from the Food Industry Research and Development Institute (Hsinchu, Taiwan). U-2 OS cells were cultured in 75 cm^2 tissue culture flasks with 90% McCoy's 5a medium containing 1.5 mM L-glutamine adjusted to 1.5 mg/l sodium bicarbonate and supplemented with 10% FBS and 1% penicillin-streptomycin (100 U/ml penicillin G and 100 μg/ml streptomycin) at 37°C under a humidified 5% CO$_2$ atmosphere, as previously described (33-36).

Cell viability assay. To evaluate the cytotoxicity of HMJ-30 in osteocarcinoma U-2 OS cells, an MTT assay was performed. Briefly, viable cells were counted on a Neubauer chamber with a microscope. U-2 OS cells were placed in a 96-well cell culture plate at an initial concentration of 1x10^5 cells/ml, and treated with HMJ-30 at different concentrations (0, 5, 10, 20, and 40 μM) or with 0.1% DMSO for 24 h at 37°C. Following a 24 h incubation period, MTT solution (0.5 mg/ml) was added to each well for 4 h at 37°C. Subsequently, the culture medium was removed, and the formazan crystals formed by oxidation of the MTT solution were dissolved with DMSO in isopropanol and measured spectrophotometrically at 490 nm. The cell survival ratio was expressed as a percentage of the control, as previously described (37-39).

Phase-contrast microscopy of morphological changes. U-2 OS cells were cultured in 24-well plates at a density of 2.5x10^5 cells/well/ml prior to treatment with 20 μM HMJ-30. Following treatment with HMJ-30 for 24 h at 37°C,

morphological changes were determined using a phase-contrast microscope (x200 and x400) as previously described (6).

Wound healing assay. To determine cell migration, U-2 OS cells were placed in a 6-well tissue culture plate for 24 h and grown to 80-90% confluence. Individual wells were scratched with a micropipette tip to create a denuded zone of constant width (1 mm). Cells were then cultured in serum-free McCoy's 5a medium and incubated with 0, 5, 10, 20, and 40 μM of HMJ-30 or with 0.1% DMSO for 24 h at 37°C. Cells were photographed under phase-contrast microscopy (x100) as previously described (35,40,41).

Transwell assay. Cell invasion was measured using a Matrigel-coated invasion chamber. Initially, a 24-well Transwell insert with 8 μm porosity polycarbonate filters (EMD Millipore) recoated with 30 μg Englebreth-Holm-Swarm sarcoma tumor matrix (EHS Matrigel Basement Membrane Matrix) at 25°C for 1 h to form a genuine reconstituted basement membrane. Cells were then maintained for 24 h in serum-free McCoy's 5a medium. The serum-starved cells were then re-suspended in serum-free medium and placed in the upper chamber of the Transwell insert (5x10^4 cells/well) and treated with different concentrations of HMJ-30 (0, 5, 10, 20 and 40 μM) or with 0.1% DMSO for 24 h at 37°C. The culture medium supplemented with 10% FBS was added to the lower chamber. The cells were then incubated at 37°C in a humidified atmosphere with 95% air and 5% CO$_2$ to allow sufficient time for invasion. Following

incubation for 24 h, the cells were fixed with 4% formaldehyde for 15 min in phosphate-buffered-saline (PBS) and stained with 2% crystal violet for 5 min at room temperature. Finally, the non-invading cells in the top well were removed with a cotton swab, and the invading cells which penetrated through the Matrigel to the bottom wells were counted under a light microscope (x200) as previously described (6,36,42).

Gelatin zymography. To determine the activity of MMP-2 and MMP-9, gelatin zymography was used. Briefly, U-2 OS cells were treated with HMJ-30 at different concentrations (0, 5, 10, 20 and 40 μM) or with 0.1% DMSO for 24 h at 37˚C in the absence of serum. Cells were then collected and separated by dilution in a zymography sample buffer. Samples were mixed with loading buffer and electrophoresed on 10% sodium dodecyl sulfate (SDS)-polyacrylamide gel with 0.1% gelatin. Gels were washed twice in denaturing buffer (2.5% Triton X-100 in double-distilled H_2O), and incubated with development buffer (50 mM Tris, pH 7.5, 200 mM NaCl, 5 mM $CaCl_2$, 1 mM $ZnCl_2$, 0.02% Briji-35) at 37˚C for 18 h, stained with 0.5% Coomassie blue G-250 for 1 h, and de-stained with de-staining solution. Non-staining bands indicating proteolytic activities were digitized using a scanning digital system and analyzed using NIH image software. MMP-2 (72-62 kDa) and MMP-9 (92-85 kDa) activity was expressed as the ratio to MMP-2 standard to avoid differences among gels (43).

Molecular modeling of the HMJ-30-protein complex. The crystal structure of the IGF-1R kinase domain complexed with a benzimidazole (Protein Data Bank code = 2oj9) was retrieved from the Protein Data Bank (http://www.rcsb. org/pdb). Automated docking was then performed. LigandFit, within the software package Discovery Studio 2.5 (Accelrys, San Diego, CA, USA) was used to evaluate and predict the *in silico* binding free energy of the inhibitors within the macromolecules. First, the prepare protein protocol was used to prepare the 2oj9 protein structure, including standardizing atom names, inserting missing atoms in residues and removing alternate conformations, inserting missing loop regions based on SEQRES data, optimizing short and medium size loop regions with Looper Algorithm, minimizing the remaining loop regions, and calculating pK and protonate structure. A binding pocket of the native benzimidazole ligand was selected as the binding site for the present study. Following typing of the receptor model with the CHARMm forcefield, the binding site was identified by the LigandFit flood-filling algorithm. This docking protocol employed total ligand flexibility, whereby the final ligand conformations were determined by the Monte Carlo conformation search method set to a variable number of trial runs. The docked ligands were further refined using *in situ* ligand minimization with the Smart Minimizer algorithm. Each minimization was performed in two steps, first using the steepest descent minimization for 200 cycles and then using conjugate gradient minimization, until the average gradient fell below 0.01 kcal/mol. All atoms within 6.0 Å of the inhibitor were allowed to relax during the minimization, whereas those atoms beyond 6.0 Å were held rigid. Finally, the Dock score was used to estimate the binding free energies of the ligands. Among the docked conformations, the pose with the highest value of Dock score was selected for the calculation of binding free energy (ΔGb) and inhibition constant (Ki).

Tyrosine kinase assay. An assay to determine tyrosine kinase activity was performed according to the manufacturer's protocols (Tyrosine kinase assay kit; EMD Millipore). U-2 OS cells were plated in 12-well plates at an initial density of 5.0×10^6 cells and incubated with 0, 20 or 40 μM of HMJ-30 or with 10 μM picopodophyllotoxin (PPP) (Sigma-Aldrich; Merck KGaA) for 6 h at 37˚C. Cells were harvested and total proteins were collected under non-denaturing conditions. Samples were incubated with tyrosine kinase reaction buffer for 30 min at 30˚C, followed by the addition of p-tyrosine (4G10) antibodies at a 1:5,000 dilution for 3 min at room temperature, and then detected using an ELISA reader (Anthos 2001) (Anthos Labtec Instruments GmbH, Salzburg, Austria) at a 450 nm wavelength, as previously described (44).

Phosphorylated protein kinase sandwich ELISA assay. p-IGF-1R β (Tyr1131) (cat. no. 7302), p-p38 MAPK (Thr180/Tyr182) (cat. no. 7946), p-p44/42 MAPK (Thr202/ Tyr204) (cat. no. 7177), and p-Akt (Thr308) (cat. no. 7252) assays were performed according to the manufacturer's protocols (PathScan Sandwich ELISA kits; Cell Signaling Technology, Inc.). In total, ~1×10^7 U-2 OS cells/ml were plated on 24-well plates and treated with 0, 20 or 40 μM of HMJ-30 or with specific protein kinase inhibitors (10 μM PPP, U0126, SB203580 or wortmannin; Sigma-Aldrich; Merck KGaA) for 6 h at 37˚C. These cells were harvested and total proteins were collected. Samples were incubated in appropriate antibody-coated microwells for 2 h at 37˚C or overnight at 4˚C. To each well, 100 μl of the appropriate antibody was added for 1 h at 37˚C, and HRP-linked secondary antibody was added for 30 min at 37˚C. Absorbance was measured with an ELISA reader (Anthos 2001) at a wavelength of 450 nm as previously described (45).

Immunoprecipitation of IGF-1R and IR proteins. U-2 OS cells were seeded in a 10-cm dish at an initial concentration of 1.0×10^7 cells and treated with 20 or 40 μM HMJ-30 or with 0.1% DMSO for 6 h. Cells were then harvested and total proteins were collected using PRO-PREP Protein Extraction Solution (iNtRON Biotechnology, Seongnam, Korea). Samples were incubated with IGF-1R or IR antibodies overnight at 4˚C, followed by adding A/G-agarose beads with gentle rocking for 3 h at 4˚C. Following centrifugation at 300 x g for 10 min at 4˚C, the pellets were washed with 1X cell lysis buffer and re-suspended in 3X SDS sample buffer. These samples were subjected to 10% SDS gel electrophoresis followed by incubation with p-tyrosine (4G10) or p-IGF-1R β (Tyr1131)/IRβ (Tyr1146) antibodies at a 1:1,000 dilution overnight at 4˚C to measure specific protein levels, as previously described (45).

Immunostaining and confocal laser microscopy. U-2 OS cells (5×10^4 cells/well) plated on a 4-well chamber slide were treated with 20 μM HMJ-30 or with 0.1% DMSO for 24 h. Cells were then fixed in 4% ice formaldehyde for 5 min at room temperature and placed in 1% bovine serum albumin (Sigma-Aldrich; Merck KGaA) containing 0.1% Triton X-100 at 37˚C for 30 min. Subsequently, the cells were washed twice

with PBS for 5 min and incubated with primary antibodies against E-cadherin (1:250 dilution), β-catenin (1:250 dilution), fibronectin (1:250 dilution), and vimentin (1:250 dilution) overnight at 4˚C and then exposed to specific secondary antibodies [fluorescein isothiocyanate-conjugated goat anti-mouse (cat. no. 31569) or anti-rabbit (cat. no. 31635) IgG antibodies; Invitrogen; Thermo Fisher Scientific] at a 1:500 dilution for 1 h at room temperature, followed by DNA staining with PI. Photomicrographs were obtained using a Leica TCS SP2 confocal spectral microscope (Leica Microsystems GmbH, Wetzlar, Germany) as previously described (46,47).

Western blotting. To analyze the expression of proteins associated with invasiveness, western blot analysis was performed. Briefly, the U-2 OS cells were plated in 10 cm-dish at an initial concentration of 1.0×10^7 cells and treated with HMJ-30 at different concentrations (0, 10, 20, and 40 μM) or with 0.1% DMSO for 6 or 24 h at 37˚C. Cells were harvested and total proteins were collected using PRO-PREP Protein Extraction Solution (iNtRON Biotechnology). Protein samples were quantified using the Pierce bicinchoninic acid (BCA) Protein assay kit (Pierce; Thermo Fisher Scientific). Samples (40 μg) were electrophoresed by 10% SDS-polyacrylamide gel electrophoresis and transferred onto nitrocellulose membranes (Invitrogen; Thermo Fisher Scientific). The membranes were then incubated in blocking solution (0.1% Tween-20 in PBS plus 5% powdered non-fat milk) for 1 h at room temperature, and incubated overnight at 4˚C with each of the indicated primary antibodies [MMP-9, MMP-2, TIMP-1, TIMP-2, E-cadherin, β-catenin, vimentin, fibronectin, Ras, p-ERK, ERK, p-JNK, JNK, p-p38, p38, PI3K (p85), p-AKT, AKT, IKK, p-IκB, IκB, NF-κB (p65), β-actin and α-tubulin] (1:1,000 dilution) diluted in blocking solution. Subsequently, the membranes were washed with PBST three times for 10 min and incubated with the appropriate HRP-conjugated secondary IgG antibodies (1:10,000 dilution; HRP-conjugated goat anti-rabbit and goat anti-mouse IgG) for 1 h at room temperature and then washed three times in PBST. Bands were detected using enhanced chemiluminescence with ECL reagents (GE Healthcare Life Sciences, Little Chalfont, UK) and exposed to X-OMAT AR films (Kodak, Rochester, NY, USA). The auto-radiograms were scanned on a UMAX PowerLook Scanner (UMAX Technologies, Fremont, CA, USA) with Photoshop CS5 software (Adobe Systems, Inc., San Jose, CA, USA), as previously described (43,48).

Analysis of NF-κB binding using an electrophoretic mobility shift assay (EMSA). Nuclear proteins were extracted from U-2 OS cells following treatment with 20 μM HMJ-30 or 10 μM ammonium pyrrolidinedithiocarbamate (PDTC; NF-κB inhibitor) (Sigma-Aldrich; Merck KGaA) for 12 h at 37˚C using the NE-PER Nuclear and Cytoplasmic Extraction Reagents kit (Pierce; Thermo Fisher Scientific, Inc.). The protein concentrations were determined using the Pierce BCA Protein assay kit (Pierce; Thermo Fisher Scientific), and biotin end-labeled oligonucleotide sequences (5'-Biotin-GATCCAGG GGACTTTCCCTAGC-3') corresponding to the consensus site of NF-κB were designed. Nuclear extract proteins (5 μg) were used for EMSA with a LightShift Chemiluminescent EMSA kit (Pierce; Thermo Fisher Scientific, Inc.) according to the

manufacturer's protocol. Biotin end-labeled duplex DNA was incubated with a nuclear extract or purified factor and electrophoresed on a 6% non-denaturing polyacrylamide native gel. For competition experiments, a 100-fold excess of unlabeled double-stranded oligonucleotide was added to the reaction. Then, the DNA was rapidly transferred to a positively-charged nitrocellulose membrane, UV cross-linked and probed with streptavidin-HRP conjugate (1:300 dilution) with gentle agitation for 15 min at room temperature. Bands were detected by enhanced chemiluminescence with ECL reagents (GE Healthcare Life Sciences) and exposed to X-OMAT AR films (Kodak) as previously described (35,49).

Statistical analysis. All data were expressed as the mean ± standard deviation from three separate experiments. Statistical analysis was performed using one-way analysis of variance followed by Dunnett's test, with SPSS software version 16.0 (SPSS, Inc., Chicago, IL, USA). $^*P<0.05$ was considered to indicate a statistically significant difference.

Results

HMJ-30 selectively targets insulin-like growth factor 1 receptor (IGF-1R). Our group synthesized a series of quinazoline derivatives targeting tyrosine kinase signaling to inhibit tumor invasion and migration. One of these compounds, HMJ-30 (Fig. 1A), was proposed to actively target IGF-1R. This hypothesis was tested using western blotting, immune-precipitation, kinase activity assays and a computational modeling program. HMJ-30 reduced protein levels of p-IGF-1R (Tyr 1131) and p-tyrosin (4G10) which are determined by immune-precipitation and western blotting (Fig. 1B). Several small molecule inhibitors of IGF-1R tyrosine kinases have been developed and they are currently undergoing clinical investigations (50). However, this approach may be unsatisfactory as co-inhibition of IR is expected to cause hyperglycemia, and this potential effect results from a high protein sequence similarity between the kinase domains of IGF-1R and IR (51). In the present study, p-IR and p-tyrosine (4G10) protein expression levels were evaluated using immune-precipitation and western blotting, and the results revealed that there was no statistical significance between HMJ-30-treated groups and the control (Fig. 1C). The effects of HMJ-30 on p-IGF-1R (Tyr1131) and tyrosine kinase in U-2 OS cells were further investigated. p-IGF-1R (Tyr1131) protein expression was significantly downregulated (Fig. 1D). Tyrosine kinase activity was significantly downregulated, as measured using a kinase assay (Fig. 1E). PPP, which has been reported to act as a non-competitive, potent and specific inhibitor of IGF-1R *in vitro* and *in vivo* (52), was used as a positive control, and was also revealed to reduce kinase activity.

Molecular modeling of HMJ-30 and IGF-1R interaction. In order to predict the major target site of HMJ-30, a docking simulation of HMJ-30 and IGF-1R was performed using the program Discovery Studio Modeling 2.5 (Accelrys). The three-dimensional crystalline structure of the IGF-1R kinase domain in complex with a benzimidazole was downloaded from the RCSB Protein Data Bank website. The computational modeling of the HMJ-30 and IGF1R interaction indicated that
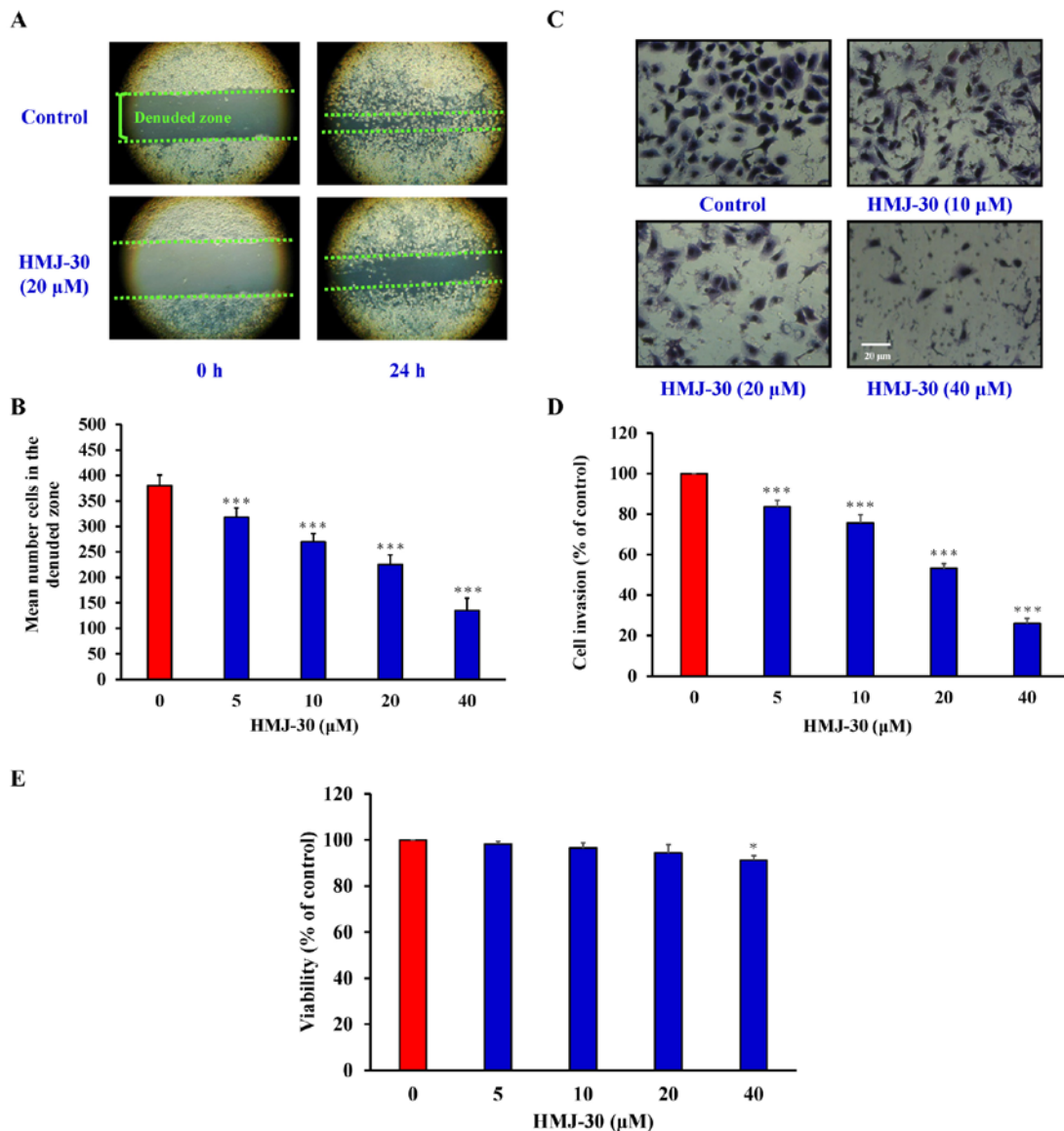
Figure 2. HMJ-30 suppresses invasion and migration in human osteogenic sarcoma U-2 OS cells. (A) Following incubation with 0, 5, 10, 20, and 40 μM HMJ-30 for 24 h in serum-free medium, cells were photographed, and (B) migrated cells were quantified. (C) The invasion of U-2 OS cells was measured using Matrigel-coated invasion chambers. Following treatment with the indicated concentrations of HMJ-30 and incubation for 24 h, the invading cells which penetrated through the Matrigel to the bottom wells were counted under a light microscope (x200), and (D) cell invasion was quantified. (E) Following treatment with 0, 5, 10, 20, and 40 μM HMJ-30 for 24 h, the cell viability of U-2 OS cells was evaluated. The data represents the mean ± standard deviation of three experiments. *P<0.05 and ***P<0.001 vs. 0 μM. HMJ-30, 6-fluoro-2-(3-fluorophenyl)-4-(cyanoanilino)quinazoline.

HMJ-30 is able to bind to the ATP-binding site of IGF-1R. The interaction between HMJ-30 and IGF-1R is involved in the F-H interaction of 6-fluoro with Ile[1130], the F-H interaction of 2-(3-fluoro) phenyl with Met[1052] and Ala[1001], the hydrophobic interactions of the quinazoline ring with Met[1126] and Thr[1127,] and the hydrophobic interactions of 2-(3-fluoro)phenyl with Met[1049] and Glu[1050] (Fig. 1F). These interactions made HMJ-30 bind readily to IGF-1R, with low potential energy. Furthermore, the structure of HMJ-30 superimposes well onto the benzimidazole inhibitor (A)-3-[(5-(1H-imidazol-1-yl)-7-methyl-1H- benzimidazol-2-yl)-4- [(pyridin-2-yl-methyl) amino]pyridin-2(1H)-one (Fig. 1F, bottom). Therefore, HMJ-30 may be an IGF-1R inhibitor.

HMJ-30 inhibits invasion in U-2 OS cells. To determine the effect of HMJ-30 on U-2 OS cell invasion, wound and Transwell assays were used. HMJ-30 inhibited cell migration in a concentration-dependent manner (Fig. 2A and B). HMJ-30 also inhibited cell invasion in a concentration-dependent manner (Fig. 2C and D). Tumor cell viability was inhibited, however, only following treatment with 40 μM HMJ-30 for 24 h (Fig. 2E). These data suggested that a concentration of HMJ-30 <40 μM primarily inhibited tumor migration and invasion, but toxicity in U-2 OS cells may require a higher concentration and an increased incubation time.

HMJ-30 inhibits MMP-2 and MMP-9 protein activity and expression levels in U-2 OS cells. Previous studies have reported that tumor invasion requires the degradation of basement membranes and proteolysis of the extracellular matrix (ECM) (4). Multiple proteolytic enzymes, including MMPs and serine proteinases, are involved in tumor-host
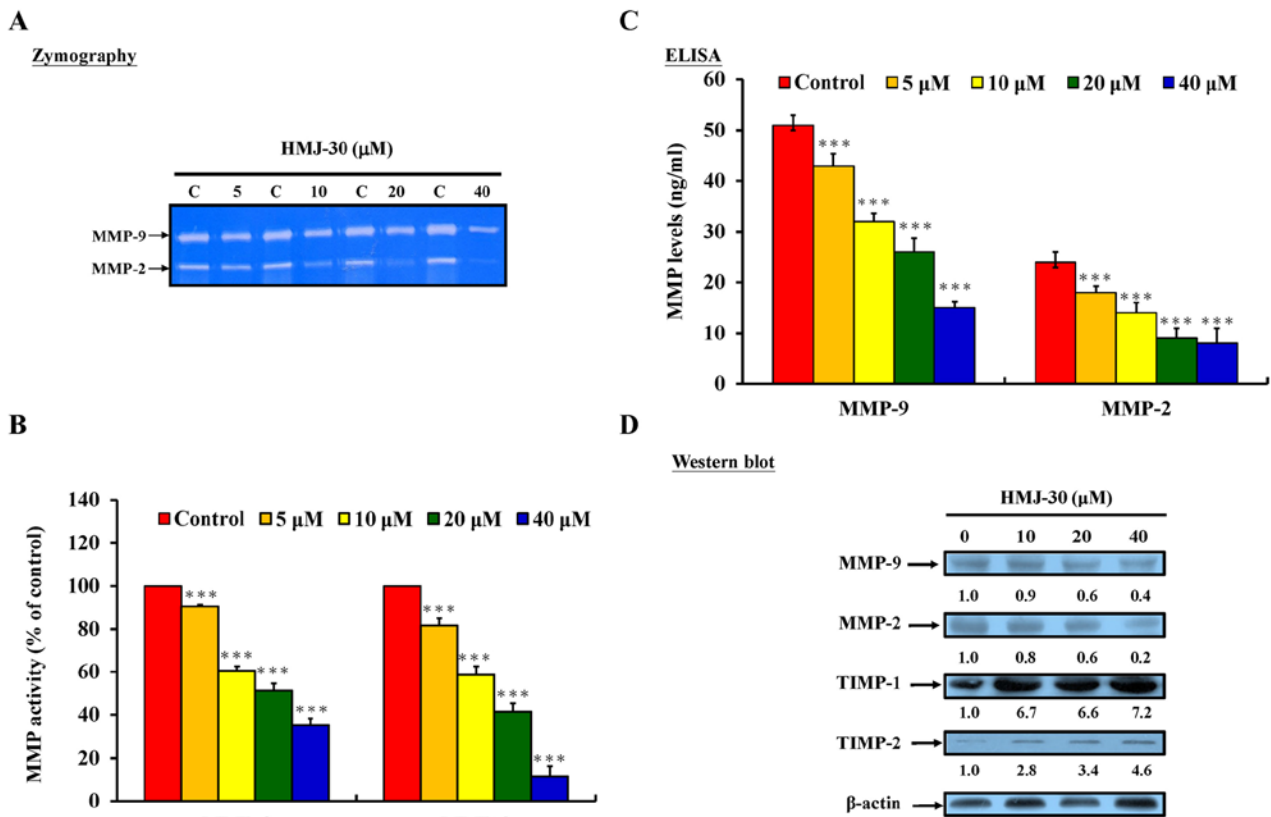
Figure 3. HMJ-30 inhibits MMP-2 and MMP-9 activity and expression levels in human osteogenic sarcoma U-2 OS cells. (A) Gelatin zymography was used to measure the activity of MMP-2 and MMP-9, and (B) MMP-9 and MMP-2 levels were quantified. (C) Following treatment with 0, 5, 10, 20 and 40 μM HMJ-30 for 24 h, MMP-9 and MMP-2 protein levels were determined by sandwich ELISA. (D) Protein levels of MMP-2, MMP-9, TIMP-1, and TIMP-2 were evaluated by western blotting. The data represents the mean ± standard deviation of three experiments. ***P<0.001 vs. control. HMJ-30, 6-fluoro-2-(3-fluorophenyl)-4-(cyanoanilino)quinazoline; MMP, matrix metalloproteinase; TIMP, tissue inhibitor of metalloproteinase.

interactions to transmigrate limiting basement membranes and the ECM (53). MMP-2 and MMP-9 serve an important function in cancer cell invasion, and degrade type IV collagen and gelatin which are primarily found in the basal lamina (54). To further evaluate the invasive activity, protein levels of MMP-2 and MMP-9 were determined by gelatin zymography, sandwich ELISA assay and western blotting. HMJ-30 significantly inhibited MMP-2 and MMP-9 activity (Fig. 3A and B) and protein levels (Fig. 3C and D).

The tissue inhibitors of metalloproteinase (TIMP) family, which includes TIMP-1 to TIMP-4, is a group of endogenous MMP inhibitors that serve a central post-translational regulatory role in the majority of known MMPs (55). TIMP-1, the inducible form, has been identified as an inhibitor of the majority of metalloproteinases. TIMP-2, a primarily constitutive protein, has been observed interacting with MMP-1, -2, -9 and -14 (55,56). The present study evaluated the protein levels of TIMP-1 and TIMP-2, which were revealed to be significantly increased in HMJ-30-treated U-2 OS cells (Fig. 3D). These results suggested that HMJ-30 may also be involved in the regulation of MMP-2 and MMP-9 activity.

HMJ-30 induces morphological changes and inhibits EMT in U-2 OS cells. During the progression and invasion of solid tissue epithelial cancers, tumor cells will lose their epithelial characteristics and gain mesenchymal properties, thus undergoing EMT (23). In contrast, previous studies have reported that the reactivation of epithelial characteristics and the loss of mesenchymal cell markers causes cells to undergo a reverse EMT process, which is also known as MET. The reverse process has been revealed to be associated with the inhibition of invasion and migration in cancer cells (57-59). To evaluate whether or not HMJ-30 induces MET in U-2 OS cells, morphological changes and mesenchymal/epithelial cell markers were investigated. HMJ-30-treated U-2 OS cells acquired a flattened, less elongated and cobblestone-like shape, which is typical of epithelial cell appearance (Fig. 4A). Furthermore, the cells were more aggregated and formed tighter clusters compared with the control group. Expression of vimentin and fibronectin (mesenchymal markers) and of E-cadherin and β-catenin (epithelial markers) were evaluated by immunofluorescent staining and western blotting. HMJ-30-treated U-2 OS cells gained E-cadherin and β-catenin (epithelial markers) and lost vimentin and fibronectin protein (mesenchymal markers) (Fig. 4B and C). These results indicated that MET acts as an important anti-invasive function in HMJ-30-treated U-2 OS cells.

HMJ-30 inhibits invasiveness through IGF-1R-mediated Ras/MAPK, PI3K/AKT and NF-κB signaling pathways in U-2 OS cells. Activated IGF-IR initiates signaling through two primary cascades, the PI3K/AKT and Ras/MAPK pathways (7). These cascades serve critical functions in diverse cellular processes (60). MAPKs are part of a phosphorylation

A

x200

x400

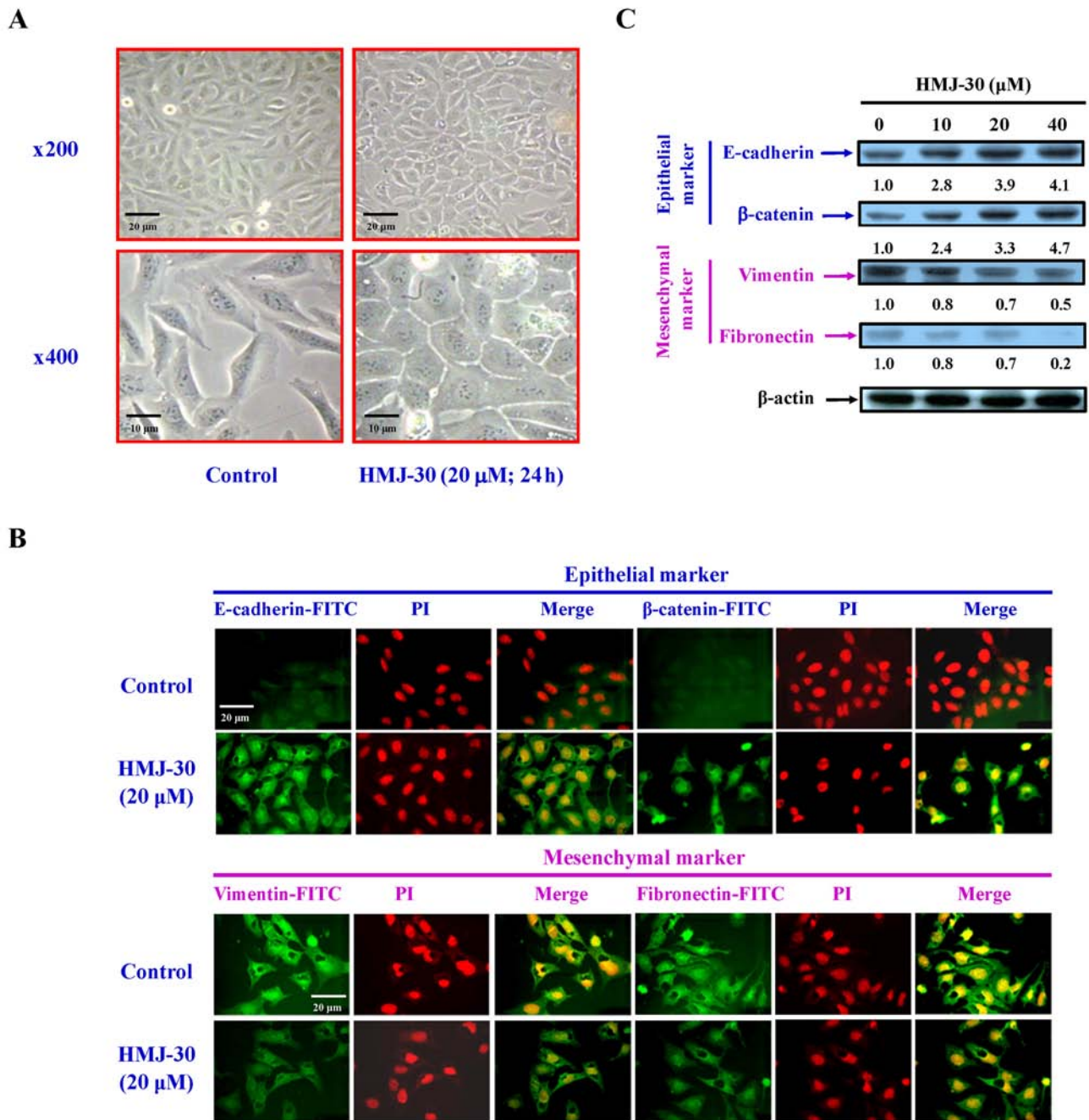Control   HMJ-30 (20 µM; 24 h)

C

B

Figure 4. HMJ-30 alters cell morphology and inhibits epithelial-mesenchymal transition in human osteogenic sarcoma U-2 OS cells. (A) Following treatment with 0 and 20 μM HMJ-30 for 24 h, cells were photographed using phase-contrast microscopy. U-2 OS cells were scattered; however, HMJ-30-treated cells were more aggregated and formed tight clusters (top, x200). The U-2 OS cells had spindle-like morphology; however, HMJ-30-treated cells gained flattened, less elongated and cobblestone-like shapes (bottom, x400). (B) Epithelial markers (E-cadherin and β-catenin; top) and mesenchymal markers (vimentin and fibronectin; bottom) were evaluated by immunofluorescent staining. (C) The protein levels of E-cadherin, β-catenin, vimentin and fibronectin were evaluated by western blotting. HMJ-30, 6-fluoro-2-(3-fluorophenyl)-4-(cyanoanilino)quinazoline; E-cadherin, epithelial cadherin.

regulatory system composed of three sequentially activated kinases, ERK1/2, p38 kinase and c-Jun amino-terminal kinases (JNKs) (60). To elucidate the potential molecular signaling pathways in HMJ-30-treated U-2 OS cells, the levels of associated proteins in the PI3K/AKT and Ras/MAPK signaling pathways were assessed using western blotting. Key phosphorylated proteins in these signaling pathways were reconfirmed via sandwich ELISA assay. HMJ-30 caused a decrease in the protein levels of Ras, p-ERK1/2, p-p38, and p-JNK in U-2 OS cells (Fig. 5A). Inhibitors of MEK 1 and

MEK 2 (U0126) and p38 (SB203580) also reduced the protein levels of p-p44/22 MAPK (ERK) and p-p38, respectively (Fig. 5B and C). HMJ-30 caused a decrease in the protein levels of PI3K (p85) and p-AKT in U-2 OS cells (Fig. 5D). Inhibitors of PI3K (wortmannin) also reduced the protein expression of p-AKT (Fig. 5E).

The PI3K and AKT signaling pathway allows the translocation of NF-κB to the nucleus to regulate gene transcription. The accumulation of IκB, resulting from the decrease of the phosphorylation of IκB by IKKs, prevents the translocation of
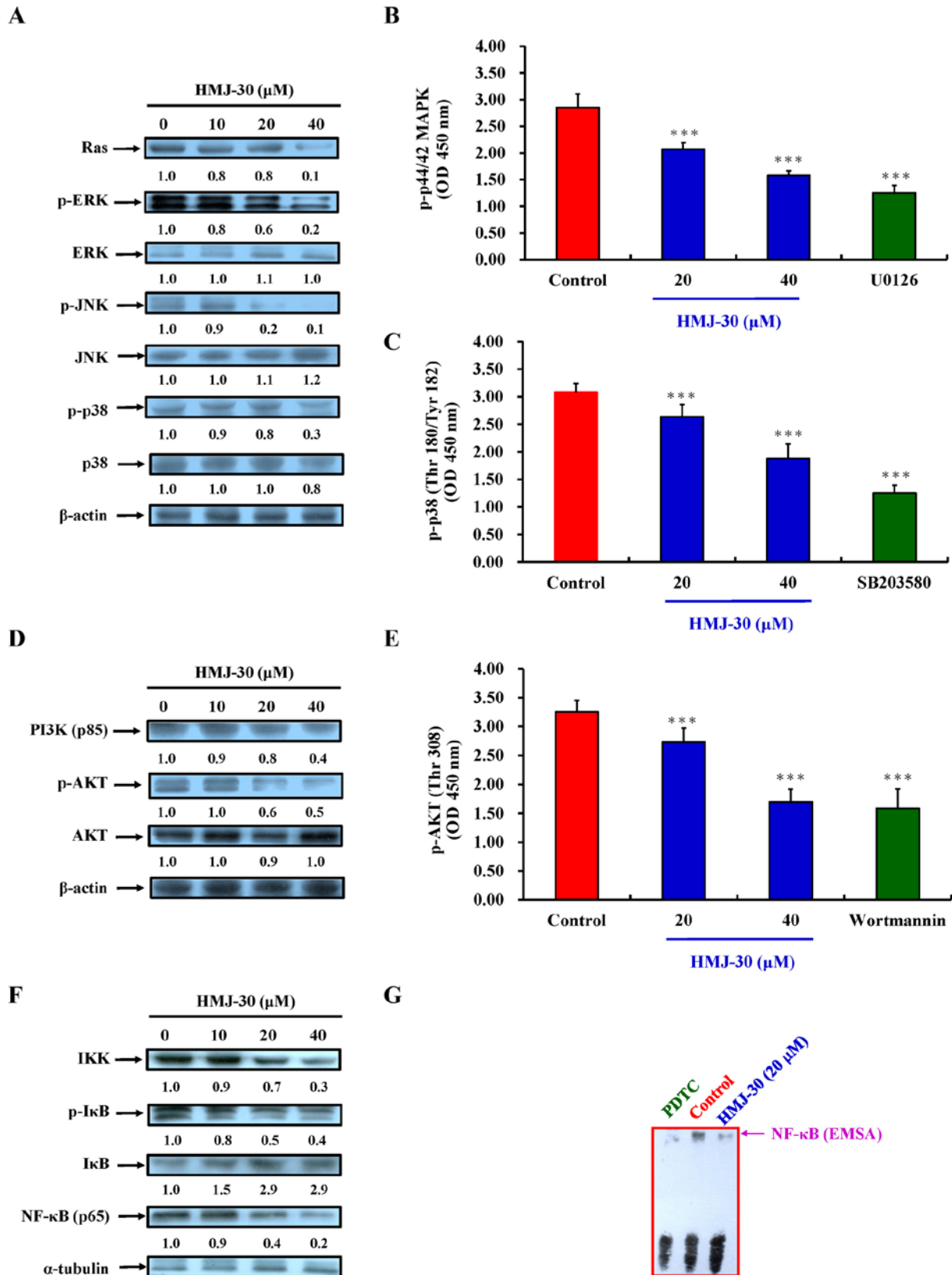
Figure 5. HMJ-30 inhibits the Ras/MAPK, PI3K/AKT, and NF-κB signaling pathways in human osteogenic sarcoma U-2 OS cells. (A) Protein levels of Ras, p-ERK, p-JNK and p-p38 were downregulated, as determined by western blotting. Expression of the key proteins in MAPK signaling, (B) p-ERK (p-p44/42) and (C) p-p38, were reconfirmed using ELISA assays. (D) The protein levels of PI3K (p85) and p-AKT were downregulated, as determined by western blotting. (E) The key protein in p-AKT was reconfirmed by ELISA assay. (F) Protein levels of IKK, p-IκB and NF-κB (p65) were downregulated, as determined by western blotting. (G) NF-κB binding activity was determined using an electrophoretic mobility shift assay. Inhibitors of p44/22 MAPK (U0126), p38 (SB203580), PI3K (wortmannin) and NF-κB (PDTC), as positive controls, reduced protein kinase levels. The data represents the mean ± standard deviation of three experiments. ***P<0.001 vs. control. HMJ-30, 6-fluoro-2-(3-fluorophenyl)-4-(cyanoanilino)quinazoline; MAPK, mitogen-activated protein kinase; PI3K, phosphoinositide 3-kinase; AKT, protein kinase B; NF-κB, nuclear factor-κB; p-, phosphorylated; ERK, extracelullar signal-regulated kinase; JNK, c-Jun amino-terminal kinase; PDTC, ammonium pyrrolidinedithiocarbamate.
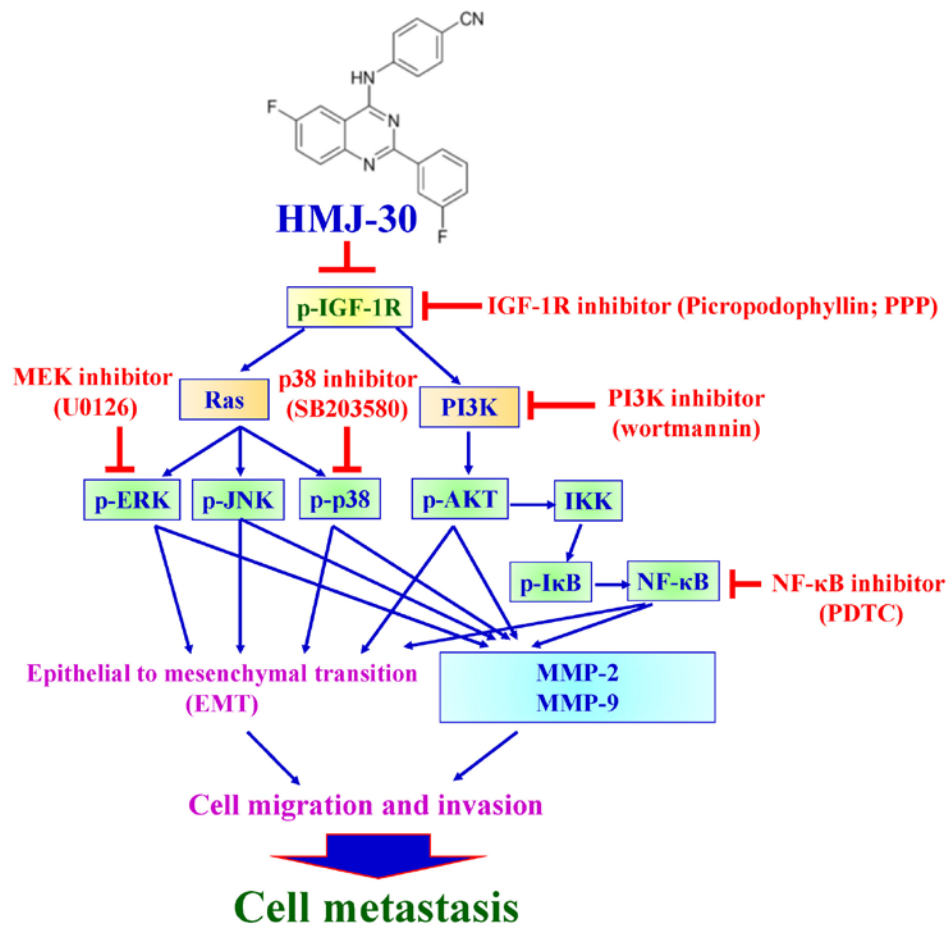
Figure 6. The proposed signaling pathways underlying HMJ-30-induced inhibition of invasiveness and EMT in human osteogenic sarcoma U-2 OS cells. HMJ-30, 6-fluoro-2-(3-fluorophenyl)-4-(cyanoanilino)quinazoline; EMT, epithelial-mesenchymal transition; p-, phosphorylated; IGF-1R, insulin-like growth factor 1 receptor; PI3K, phosphoinositide 3-kinase; ERK, extracelullar signal-regulated kinase; JNK, c-Jun amino-terminal kinase; AKT, protein kinase B; MMP, matrix metalloproteinase.

NF-κB and the activation of transcription by retaining NF-κB in the cytoplasm (61). NF-κB serves an important function in the modulation of the expression of oncogenes, including MMP-2/9, cyclin D1, cell survival proteins and vascular endo-thelial growth factor; the activities of which are associated with the growth as well as the invasive and metastatic propertoes of cancer cells (61,62). HMJ-30 caused a decrease in protein levels of IKK and NF-κB (p65) and an increase in the protein level of IκB, as confirmed by western blotting (Fig. 5F). HMJ-30 caused a decrease in the protein levels of IKK and NF-κB (p65) and an increase in the protein levels of IκB (Fig. 5F). Furthermore, HMJ-30 caused a decrease in NF-κB activity, and the inhibitor of NF-κB, PDTC, also reduced the activity of NF-κB, as determined by EMSA (Fig. 5G). These results suggested that HMJ-30 inhibited PI3K/AKT, Ras/MAPK, and IκB/NF-κB signaling pathways in U-2 OS cells.

Discussion

Several quinazoline derivatives have been developed to act as potent and selective inhibitors of the growth factor receptor tyrosine kinase (25). The quinazoline ring has been reported to occupy the adenine binding site of the tyrosine kinase receptor, and to inhibit its phosphorylation. Anilinoquinazolines have also been reported to act as potent therapeutic agents in invasive cancers to prevent metastasis (27). Our group has designed and synthesized several anilinoquinazolines in order to inhibit tumor metastasis. One of these compounds, HMJ-30 (Fig. 1A), selectively targeted the ATP binding site of IGF-1R and downregulated MAPKs, as well as PI3K/AKT signaling. In order to gain further insights into HMJ-30 inhibiting the IGF-1R signaling pathway in human osteosar-coma, the antitumor effects in HMJ-30-treated U-2 OS cells were evaluated. The U-2 OS cell line, with its spindle-like morphology (Fig. 4A), was established by Ponten and Saksela from the osteosarcoma of a 15-year old Caucasian female (63). *In vitro* studies have demonstrated that U-2 OS cells grow via autocrine stimulation by expressing IGF-IR and insulin-like growth factor-II/mannose-6-phosphate (IGF-II/M6P) recep-tors, and synthesizing and secreting IGF-like peptides (13). Initially, migration and invasion were evaluated in HMJ-30-treated U-2 OS cells. HMJ-30 inhibited cell migration and invasion in a concentration-dependent manner (Fig. 2). These results are in agreement with a previous study *in vitro* which revealed that the downregulation of endogenous IGF-1R expression by lentivirus-mediated RNAi reduces tumor inva-sion in osteosarcoma cells (14). The present study revealed that <40 μM HMJ-30 inhibited tumor migration and invasion; whereas a higher concentration and an increased incubation time induced toxicity in U-2 OS cells.

The degradation of basement membranes and the proteolysis of the ECM has been reported to enable tumors to migrate into adjacent tissues or transmigrate, limiting basement membranes and extracellular matrices (4). MMPs are zinc-dependent endopeptidases and serve a major function in ECM degradation and remodeling. Previous studies have demonstrated that overexpression of MMPs, particularly the gelatinases MMP-2 and MMP-9, is associated with the invasive properties of several tumor cell lines (54,64). The results of the present study demonstrated that HMJ-30 decreased the protein activities and levels of MMP-2 and MMP-9 in U-2 OS cells (Fig. 3).

Regulation of MMPs consists of three levels: i) gene expression; ii) activation of the latent pro-enzymes; and iii) inhibition by tissue inhibitor of metalloproteinases (TIMPs) (4,54,60,66). MMP gene expression at the transcriptional and post-transcriptional levels is regulated through multiple signaling pathways, and is directed by the protein kinases (60). Highly selective inhibitors of PI3K (wortmannin), MEK (U0126), p38 MAPK (SB203580) and JNK (SP600125) confirm the regulation of MMP gene expression by the PI3K/AKT and Ras/MAPK pathways (60). The transcription factor, NF-κB, has binding sites in the promoter of MMPs genes, including MMP-2 and -9. PDTC, an inhibitor of NF-κB, determined the modulation of MMP production (60,62). In a recent study, IGF-1R signaling was reported to act as a positive and negative regulator of MMP expression and function (64). Based on previous studies and present results, it would appear that HMJ-30 suppressed MMP-2 and MMP-9 expression through IGF-1R-mediated PI3K/AKT and Ras/MAPK signaling pathways in U-2 OS cells. On the other hand, the upregulation of TIMP-1 and TIMP-2 suggests that HMJ-30 may be involved in post-translational regulation of MMP activity. Normally, the expression of the majority of MMPs is low in tissue; however, as it is required for remodeling ECM, it is induced by several extracellular stimuli (60). MMPs in human cancers have functions beyond ECM degradation. They induce cancer cells to produce numerous growth factors, cytokines and chemokines which contribute to the expression of MMPs by stromal cells, creating a favorable environment for metastasis (53). The present study indicated that the upregulation of TIMP-1 and TIMP-2 by HMJ-30 may not only inhibit MMPs produced by U-2 OS cells, but may also reduce the activity of stromal-derived MMPs.

Epithelial cells form layers kept together by specialized membrane structures which limit the movement of epithelial cells to the two-dimensional space of the epithelial plane. In contrast, mesenchymal cells only have focal contacts with their neighbors without forming organized cell layers, which are elongated and motile in a three-dimensional space, enriching MMPs (66). During cancer progression, EMT occurs in which epithelial cells lose their epithelial characteristics and gain mesenchymal properties (23). These differentiated mesenchymal cells easily spread into tissues surrounding the original tumor, as well as travelling to other locations. Finally, the disseminated tumor cells undergo a reverse EMT process, MET, recapitulating the corresponding primary tumors at the site of metastasis to establish a secondary tumor (23). Previous studies have reported that specific inhibition of tumor invasion and migration reactivates epithelial characteristics and lose mesenchymal cell markers, resulting in MET in malignancies (57-59). Pax3 has also been reported to induce the formation of multi-layered condensed cell aggregates with epithelial characteristics and regulated phenotypic mesenchymal-epithelial interconversion in osteogenic Saos-2 cells (67,68). However, few further discussions concerning the association between metastasis and MET in osteosarcoma cells have occurred. HMJ-30-treated U-2 OS cells acquired a flattened, less elongated and cobblestone-like shape, which is typical of an epithelial appearance, and underwent MET as determined by an increase of epithelial markers and a reduction of mesenchymal markers (Fig. 4).

E-cadherin is a key component of intercellular junctions, and spans membranes to hook into E-cadherin molecules on adjacent cells. β-catenin, an intracellular attachment protein, binds to the intracellular domain of E-cadherin and links E-cadherin to the intracellular cytoskeletons. The E-cadherin/β-catenin complex therefore provides the major strength underlying cell-cell associations, establishing cell polarity and supporting the cellular structure. Loss of E-cadherin and junction complex has been implicated in the gain of invasive potential by cancer cells (69). In the present study, HMJ-30 upregulated protein levels of E-cadherin and β-catenin around the cytoplasm and membrane (Fig. 4B and C). One interpretation of these results is that HMJ-30 caused tumor cell aggregation and formed tight clusters through increasing cell-cell junctions to limit the invasion and migration of these differentiated epithelial cells from the primary site.

Several transcription factors, including Snail, Slug, Twist, and zinc finger E-box binding homeobox 1 (Zeb1), are crucial to EMT. NF-κB was recently demonstrated to be essential for EMT and metastasis via binding to the Snail promoter and increasing its activity (70). Furthermore, inhibition of NF-κB prevented EMT in Ras-transformed epithelial cells and caused a reversal of EMT in mesenchymal cells, suggesting that the induction and maintenance of EMT critically depend on NF-κB activity (71). Activation of IGF-1R kinase was also reported to cause EMT and promote metastasis in prostate and breast epithelial tumors through PI3K/AKT and Ras/MAPK signaling, increasing the transcriptional actives of Snail and Zeb1 (70,72). In the present study, blockage of IGF-1R by HMJ-30 reduced NF-κB activity and downregulated PI3K/AKT and Ras/MAPK pathway signaling, resulting in MET in U-2 OS cells.

In conclusion, the present study has demonstrated that HMJ-30 inhibits tumor invasiveness and induces mesenchymal-epithelial transition via selective blockage of IGF-1R signaling, involving PI3K/AKT and Ras/MAPK pathways in human osteosarcoma U-2 OS cells. Furthermore, this occurred without targeting IR, which indicated that HMJ-30 causes fewer toxic side-effects compared with the conventional chemotherapy. Downregulated protein levels and MMP-2 and MMP-9 activity, and upregulated TIMP-1 and TIMP-2 protein levels indicated that HMJ-30 not only inhibited MMP gene expression but also acted through post-translational regulation. HMJ-30 induced dramatic morphology changes in U-2 OS cells and increased the expression of epithelial markers and reduced mesenchymal markers, suggesting that HMJ-30 treatment inhibited invasiveness in tumor cells.

The proposed signal pathways underlying HMJ-30-induced IGF-1R blockage are presented in Fig. 6. These results provide important information regarding the potential molecular mechanisms of the effect of HMJ-30 on osteosarcoma, and confirm that HMJ-30 may be a candidate osteosarcoma drug in the future.

Acknowledgements

Funding

Availability of data and materials

The data sets generated during the study are available from the corresponding author on reasonable request.

Authors' contributions

YJC, MJH and JSY conceived and designed the experiments. YAJ, CCL and TLC performed the experiments. FJT, HM and YNJ analyzed the data. YJC, MJH and JSY wrote and modified the paper. All authors read and approved the final manuscript.

Ethics approval and consent to participate

Not applicable.

Consent for publication

Not applicable.

Competing interests

The authors declare that they have no competing interests.

References

1. Arndt CA and Crist WM: Common musculoskeletal tumors of childhood and adolescence. N Engl J Med 341: 342-352, 1999.
2. Chou AJ and Gorlick R: Chemotherapy resistance in osteosarcoma: Current challenges and future directions. Expert Rev Anticancer Ther 6: 1075-1085, 2006.
3. O'Day K and Gorlick R: Novel therapeutic agents for osteosarcoma. Expert Rev Anticancer Ther 9: 511-523, 2009.
4. Wells A: Tumor invasion: Role of growth factor-induced cell motility. Adv Cancer Res 78: 31-101, 2000.
5. Duan Z, Choy E, Harmon D, Yang C, Ryu K, Schwab J, Mankin H and Hornicek FJ: Insulin-like growth factor-I receptor tyrosine kinase inhibitor cyclolignan picropodophyllin inhibits proliferation and induces apoptosis in multidrug resistant osteosarcoma cell lines. Mol Cancer Ther 8: 2122-2130, 2009.
6. Liao CL, Lai KC, Huang AC, Yang JS, Lin JJ, Wu SH, Gibson Wood W, Lin JG and Chung JG: Gallic acid inhibits migration and invasion in human osteosarcoma U-2 OS cells through suppressing the matrix metalloproteinase-2/-9, protein kinase B (PKB) and PKC signaling pathways. Food Chem Toxicol 50: 1734-1740, 2012.
7. Ullrich A, Gray A, Tam AW, Yang-Feng T, Tsubokawa M, Collins C, Henzel W, Le Bon T, Kathuria S, Chen E, *et al*: Insulin-like growth factor I receptor primary structure: Comparison with insulin receptor suggests structural determinants that define functional specificity. EMBO J 5: 2503-2512, 1986.
8. Zwick E, Bange J and Ullrich A: Receptor tyrosine kinase signalling as a target for cancer intervention strategies. Endocr Relat Cancer 8: 161-173, 2001.
9. Rowlands MA, Gunnell D, Harris R, Vatten LJ, Holly JM and Martin RM: Circulating insulin-like growth factor peptides and prostate cancer risk: A systematic review and meta-analysis. Int J Cancer 124: 2416-2429, 2009.
10. Kurmasheva RT and Houghton PJ: IGF-I mediated survival pathways in normal and malignant cells. Biochim Biophys Acta 1766: 1-22, 2006.
11. Conover CA: Insulin-like growth factor-binding proteins and bone metabolism. Am J Physiol Endocrinol Metab 294: E10-E14, 2008.
12. Johnson LC: A general theory of bone tumors. Bull N Y Acad Med 29: 164-171, 1953.
13. Raile K, Höflich A, Kessler U, Yang Y, Pfuender M, Blum WF, Kolb H, Schwarz HP and Kiess W: Human osteosarcoma (U-2 OS) cells express both insulin-like growth factor-I (IGF-I) receptors and insulin-like growth factor-II/mannose-6-phosphate (IGF-II/M6P) receptors and synthesize IGF-II: Autocrine growth stimulation by IGF-II via the IGF-I receptor. J Cell Physiol 159: 531-541, 1994.
14. Wang YH, Wang ZX, Qiu Y, Xiong J, Chen YX, Miao DS and De W: Lentivirus-mediated RNAi knockdown of insulin-like growth factor-1 receptor inhibits growth, reduces invasion, and enhances radiosensitivity in human osteosarcoma cells. Mol Cell Biochem 327: 257-266, 2009.
15. Burrow S, Andrulis IL, Pollak M and Bell RS: Expression of insulin-like growth factor receptor, IGF-1, and IGF-2 in primary and metastatic osteosarcoma. J Surg Oncol 69: 21-27, 1998.
16. Benini S, Baldini N, Manara MC, Chano T, Serra M, Rizzi S, Lollini PL, Picci P and Scotlandi K: Redundancy of autocrine loops in human osteosarcoma cells. Int J Cancer 80: 581-588, 1999.
17. Kappel CC, Velez-Yanguas MC, Hirschfeld S and Helman LJ: Human osteosarcoma cell lines are dependent on insulin-like growth factor I for in vitro growth. Cancer Res 54: 2803-2807, 1994.
18. Pinski J, Schally AV, Halmos G, Szepeshazi K and Groot K: Somatostatin analog RC-160 inhibits the growth of human osteosarcomas in nude mice. Int J Cancer 65: 870-874, 1996.
19. Mansky PJ, Liewehr DJ, Steinberg SM, Chrousos GP, Avila NA, Long L, Bernstein D, Mackall CL, Hawkins DS and Helman LJ: Treatment of metastatic osteosarcoma with the somatostatin analog OncoLar: Significant reduction of insulin-like growth factor-1 serum levels. J Pediatr Hematol Oncol 24: 440-446, 2002.
20. Yee D: Targeting insulin-like growth factor pathways. Br J Cancer 94: 465-468, 2006.
21. Boyer B, Vallés AM and Edme N: Induction and regulation of epithelial-mesenchymal transitions. Biochem Pharmacol 60: 1091-1099, 2000.
22. Thiery JP and Sleeman JP: Complex networks orchestrate epithelial-mesenchymal transitions. Nat Rev Mol Cell Biol 7: 131-142, 2006.
23. Hugo H, Ackland ML, Blick T, Lawrence MG, Clements JA, Williams ED and Thompson EW: Epithelial - mesenchymal and mesenchymal - epithelial transitions in carcinoma progression. J Cell Physiol 213: 374-383, 2007.
24. Nakaya Y, Kuroda S, Katagiri YT, Kaibuchi K and Takahashi Y: Mesenchymal-epithelial transition during somitic segmentation is regulated by differential roles of Cdc42 and Rac1. Dev Cell 7: 425-438, 2004.
25. Michael JP: Quinoline, quinazoline and acridone alkaloids. Nat Prod Rep 25: 166-187, 2008.
26. Hwang SH, Rait A, Pirollo KF, Zhou Q, Yenugonda VM, Chinigo GM, Brown ML and Chang EH: Tumor-targeting nanodelivery enhances the anticancer activity of a novel quinazolinone analogue. Mol Cancer Ther 7: 559-568, 2008.
27. Plé PA, Green TP, Hennequin LF, Curwen J, Fennell M, Allen J, Lambert-Van Der Brempt C and Costello G: Discovery of a new class of anilinoquinazoline inhibitors with high affinity and specificity for the tyrosine kinase domain of c-Src. J Med Chem 47: 871-887, 2004.

28. Hennequin LF, Stokes ES, Thomas AP, Johnstone C, Plé PA, Ogilvie DJ, Dukes M, Wedge SR, Kendrew J and Curwen JO: Novel 4-anilinoquinazolines with C-7 basic side chains: Design and structure activity relationship of a series of potent, orally active, VEGF receptor tyrosine kinase inhibitors. J Med Chem 45: 1300-1312, 2002.

29. Zhou Y, Li S, Hu YP, Wang J, Hauser J, Conway AN, Vinci MA, Humphrey L, Zborowska E, Willson JK, et al: Blockade of EGFR and ErbB2 by the novel dual EGFR and ErbB2 tyrosine kinase inhibitor GW572016 sensitizes human colon carcinoma GEO cells to apoptosis. Cancer Res 66: 404-411, 2006.

30. Al-Obaid AM, Abdel-Hamide SG, El-Kashef HA, Abdel-Aziz AA, El-Azab AS, Al-Khamees HA and El-Subbagh HI: Substituted quinazolines, part 3. Synthesis, in vitro antitumor activity and molecular modeling study of certain 2-thieno-4(3H)-quinazolinone analogs. Eur J Med Chem 44: 2379-2391, 2009.

31. Ciardiello F, Caputo R, Bianco R, Damiano V, Pomatico G, De Placido S, Bianco AR and Tortora G: Antitumor effect and potentiation of cytotoxic drugs activity in human cancer cells by ZD-1839 (Iressa), an epidermal growth factor receptor-selective tyrosine kinase inhibitor. Clin Cancer Res 6: 2053-2063, 2000.

32. Lu CC, Chen HP, Chiang JH, Jin YA, Kuo SC, Wu TS, Hour MJ, Yang JS and Chiu YJ: Quinazoline analog HMJ-30 inhibits angiogenesis: Involvement of endothelial cell apoptosis through ROS-JNK-mediated death receptor 5 signaling. Oncol Rep 32: 597-606, 2014.

33. Chiu YJ, Hour MJ, Lu CC, Chung JG, Kuo SC, Huang WW, Chen HJ, Jin YA and Yang JS: Novel quinazoline HMJ-30 induces U-2 OS human osteogenic sarcoma cell apoptosis through induction of oxidative stress and up-regulation of ATM/ p53 signaling pathway. J Orthop Res 29: 1448-1456, 2011.

34. Tsai YF, Huang CW, Chiang JH, Tsai FJ, Hsu YM, Lu CC, Hsiao CY and Yang JS: Gadolinium chloride elicits apoptosis in human osteosarcoma U-2 OS cells through extrinsic signaling, intrinsic pathway and endoplasmic reticulum stress. Oncol Rep 36: 3421-3426, 2016.

35. Chen HJ, Lin CM, Lee CY, Shih NC, Peng SF, Tsuzuki M, Amagaya S, Huang WW and Yang JS: Kaempferol suppresses cell metastasis via inhibition of the ERK-p38-JNK and AP-1 signaling pathways in U-2 OS human osteosarcoma cells. Oncol Rep 30: 925-932, 2013.

36. Chueh FS, Chen YY, Huang AC, Ho HC, Liao CL, Yang JS, Kuo CL and Chung JG: Bufalin-inhibited migration and invasion in human osteosarcoma U-2 OS cells is carried out by suppression of the matrix metalloproteinase-2, ERK, and JNK signaling pathways. Environ Toxicol 29: 21-29, 2014.

37. Ma YS, Weng SW, Lin MW, Lu CC, Chiang JH, Yang JS, Lai KC, Lin JP, Tang NY, Lin JG, et al: Antitumor effects of emodin on LS1034 human colon cancer cells in vitro and in vivo: Roles of apoptotic cell death and LS1034 tumor xenografts model. Food Chem Toxicol 50: 1271-1278, 2012.

38. Wu SH, Hang LW, Yang JS, Chen HY, Lin HY, Chiang JH, Lu CC, Yang JL, Lai TY, Ko YC, et al: Curcumin induces apoptosis in human non-small cell lung cancer NCI-H460 cells through ER stress and caspase cascade- and mitochondria-dependent pathways. Anticancer Res 30: 2125-2133, 2010.

39. Lee MR, Lin C, Lu CC, Kuo SC, Tsao JW, Juan YN, Chiu HY, Lee FY, Yang JS and Tsai FJ: YC-1 induces G0/G1phase arrest and mitochondria-dependent apoptosis in cisplatin-resistant human oral cancer CAR cells. Biomedicine (Taipei) 7: 12, 2017.

40. Yang JS, Lin CA, Lu CC, Wen YF, Tsai FJ and Tsai SC: Carboxamide analog ITR-284 evokes apoptosis and inhibits migration ability in human lung adenocarcinoma A549 cells. Oncol Rep 37: 1786-1792, 2017.

41. Tsai SC, Tsai MH, Chiu CF, Lu CC, Kuo SC, Chang NW and Yang JS: AMPK-dependent signaling modulates the suppression of invasion and migration by fenofibrate in CAL 27 oral cancer cells through NF-κB pathway. Environ Toxicol 31: 866-876, 2016.

42. Hsu SC, Yang JS, Kuo CL, Lo C, Lin JP, Hsia TC, Lin JJ, Lai KC, Kuo HM, Huang LJ, et al: Novel quinolone CHM-1 induces apoptosis and inhibits metastasis in a human osterogenic sarcoma cell line. J Orthop Res 27: 1637-1644, 2009.

43. Lai KC, Huang AC, Hsu SC, Kuo CL, Yang JS, Wu SH and Chung JG: Benzyl isothiocyanate (BITC) inhibits migration and invasion of human colon cancer HT29 cells by inhibiting matrix metalloproteinase-2/-9 and urokinase plasminogen (uPA) through PKC and MAPK signaling pathway. J Agric Food Chem 58: 2935-2942, 2010.

44. Chen HJ, Jiang YL, Lin CM, Tsai SC, Peng SF, Fushiya S, Hour MJ and Yang JS: Dual inhibition of EGFR and c-Met kinase activation by MJ-56 reduces metastasis of HT29 human colorectal cancer cells. Int J Oncol 43: 141-150, 2013.

45. Han J, Lee JD, Bibbs L and Ulevitch RJ: A MAP kinase targeted by endotoxin and hyperosmolarity in mammalian cells. Science 265: 808-811, 1994.

46. Lai WW, Hsu SC, Chueh FS, Chen YY, Yang JS, Lin JP, Lien JC, Tsai CH and Chung JG: Quercetin inhibits migration and invasion of SAS human oral cancer cells through inhibition of NF-κB and matrix metalloproteinase-2/-9 signaling pathways. Anticancer Res 33: 1941-1950, 2013.

47. Yu CS, Huang AC, Yang JS, Yu CC, Lin CC, Chung HK, Huang YP, Chueh FS and Chung JG: Safrole induces G0/G1 phase arrest via inhibition of cyclin E and provokes apoptosis through endoplasmic reticulum stress and mitochondrion-dependent pathways in human leukemia HL-60 cells. Anticancer Res 32: 1671-1679, 2012.

48. Huang WW, Chiu YJ, Fan MJ, Lu HF, Yeh HF, Li KH, Chen PY, Chung JG and Yang JS: Kaempferol induced apoptosis via endo-plasmic reticulum stress and mitochondria-dependent pathway in human osteosarcoma U-2 OS cells. Mol Nutr Food Res 54: 1585-1595, 2010.

49. Hour MJ, Tsai SC, Wu HC, Lin MW, Chung JG, Wu JB, Chiang JH, Tsuzuki M and Yang JS: Antitumor effects of the novel quinazolinone MJ-33: Inhibition of metastasis through the MAPK, AKT, NF-κB and AP-1 signaling pathways in DU145 human prostate cancer cells. Int J Oncol 41: 1513-1519, 2012.

50. Weroha SJ and Haluska P: IGF-1 receptor inhibitors in clinical trials - early lessons. J Mammary Gland Biol Neoplasia 13: 471-483, 2008.

51. Hofmann F and García-Echeverría C: Blocking the insulin-like growth factor-I receptor as a strategy for targeting cancer. Drug Discov Today 10: 1041-1047, 2005.

52. Girnita A, Girnita L, del Prete F, Bartolazzi A, Larsson O and Axelson M: Cyclolignans as inhibitors of the insulin-like growth factor-1 receptor and malignant cell growth. Cancer Res 64: 236-242, 2004.

53. Sengupta N and MacDonald TT: The role of matrix metallopro-teinases in stromal/epithelial interactions in the gut. Physiology (Bethesda) 22: 401-409, 2007.

54. Björklund M and Koivunen E: Gelatinase-mediated migration and invasion of cancer cells. Biochim Biophys Acta 1755: 37-69, 2005.

55. Brew K, Dinakarpandian D and Nagase H: Tissue inhibitors of metalloproteinases: Evolution, structure and function. Biochim Biophys Acta 1477: 267-283, 2000.

56. Wojtowicz-Praga SM, Dickson RB and Hawkins MJ: Matrix metalloproteinase inhibitors. Invest New Drugs 15: 61-75, 1997.

57. Hong KO, Kim JH, Hong JS, Yoon HJ, Lee JI, Hong SP and Hong SD: Inhibition of Akt activity induces the mesenchymal-to-epithelial reverting transition with restoring E-cadherin expression in KB and KOSCC-25B oral squamous cell carcinoma cells. J Exp Clin Cancer Res 28: 28, 2009.

58. Jo M, Lester RD, Montel V, Eastman B, Takimoto S and Gonias SL: Reversibility of epithelial-mesenchymal transition (EMT) induced in breast cancer cells by activation of urokinase receptor-dependent cell signaling. J Biol Chem 284: 22825-22833, 2009.

59. Funasaka T, Hu H, Yanagawa T, Hogan V and Raz A: Down-regulation of phosphoglucose isomerase/autocrine motility factor results in mesenchymal-to-epithelial transition of human lung fibrosarcoma cells. Cancer Res 67: 4236-4243, 2007.

60. Reuben PM and Cheung HS: Regulation of matrix metal-loproteinase (MMP) gene expression by protein kinases. Front Biosci 11: 1199-1215, 2006.

61. Sliva D: Signaling pathways responsible for cancer cell invasion as targets for cancer therapy. Curr Cancer Drug Targets 4: 327-336, 2004.

62. Clark IM, Swingler TE, Sampieri CL and Edwards DR: The regulation of matrix metalloproteinases and their inhibitors. Int J Biochem Cell Biol 40: 1362-1378, 2008.

63. Pontén J and Saksela E: Two established in vitro cell lines from human mesenchymal tumours. Int J Cancer 2: 434-447, 1967.

64. Li S, Zhang D, Yang L, Burnier JV, Wang N, Lin R, Lee ER, Glazer RI and Brodt P: The IGF-I receptor can alter the matrix metalloproteinase repertoire of tumor cells through transcrip-tional regulation of PKC-{alpha}. Mol Endocrinol 23: 2013-2025, 2009.

65. Yan C and Boyd DD: Regulation of matrix metalloproteinase gene expression. J Cell Physiol 211: 19-26, 2007.

66. Berx G, Raspé E, Christofori G, Thiery JP and Sleeman JP: Pre-EMTing metastasis? Recapitulation of morphogenetic processes in cancer. Clin Exp Metastasis 24: 587-597, 2007.
67. Wiggan O, Fadel MP and Hamel PA: Pax3 induces cell aggregation and regulates phenotypic mesenchymal-epithelial interconversion. J Cell Sci 115: 517-529, 2002.
68. Wiggan O, Shaw AE and Bamburg JR: Essential requirement for Rho family GTPase signaling in Pax3 induced mesenchymal-epithelial transition. Cell Signal 18: 1501-1514, 2006.
69. Hsu YM, Chen YF, Chou CY, Tang MJ, Chen JH, Wilkins RJ, Ellory JC and Shen MR: KCl cotransporter-3 down-regulates E-cadherin/beta-catenin complex to promote epithelial-mesenchymal transition. Cancer Res 67: 11064-11073, 2007.
70. Kim HJ, Litzenburger BC, Cui X, Delgado DA, Grabiner BC, Lin X, Lewis MT, Gottardis MM, Wong TW, Attar RM, *et al*: Constitutively active type I insulin-like growth factor receptor causes transformation and xenograft growth of immortalized mammary epithelial cells and is accompanied by an epithelial-to-mesenchymal transition mediated by NF-kappaB and snail. Mol Cell Biol 27: 3165-3175, 2007.
71. Huber MA, Azoitei N, Baumann B, Grünert S, Sommer A, Pehamberger H, Kraut N, Beug H and Wirth T: NF-kappaB is essential for epithelial-mesenchymal transition and metastasis in a model of breast cancer progression. J Clin Invest 114: 569-581, 2004.
72. Graham TR, Zhau HE, Odero-Marah VA, Osunkoya AO, Kimbro KS, Tighiouart M, Liu T, Simons JW and O'Regan RM: Insulin-like growth factor-I-dependent up-regulation of ZEB1 drives epithelial-to-mesenchymal transition in human prostate cancer cells. Cancer Res 68: 2479-2488, 2008.